Identification of multiphasic and weak-link structures in a $(La_{0.94}Sr_{0.06})_2CuO_4$ single crystal by magnetically modulated resistance

F. J. Adrian, B. F. Kim, K. Moorjani, and J. Bohandy
Milton S. Eisenhower Research Center, The Johns Hopkins University, Applied Physics Laboratory, Laurel, Maryland 20723
(Received 7 January 1991)

Magnetically modulated microwave and dc-resistance measurements on a $(La_{0.94}Sr_{0.06})_2CuO_4$ crystal show that these techniques, combined with measurement of the corresponding unmodulated resistances, constitute a simple and reliable method for examining superconductor crystals both for the presence of multiple phases with different T_c's and also for the presence of weak links between different superconducting regions. Comparison of the dc and microwave results clearly demonstrates the ability of microwave measurements to assess the experimentally important surface regions of a crystal, in contrast to dc resistance, which probes the best superconducting path through the crystal. These methods can also identify weak links and determine their orientation, as illustrated by the finding of *b*-axis-oriented weak links in the crystal.

I. INTRODUCTION

Single crystals of the high-T_c superconductors now play a key role in much of the current critical research in this field.[1] Although experiments on polycrystalline samples produced by sintering compressed mixtures of the component metal oxides have yielded important information in the past and are still useful in some cases, single crystals, or crystalline films, are essential for investigating the orientation dependences of such properties as conductivity, magnetic field dependence, etc., and they are highly desirable, if not essential, for experiments requiring well-defined surfaces. Many of the experiments deemed most likely to shed light on the electronic structure of superconducting mechanism(s) in the cuprate superconductors fall into these categories as, for example, optical and infrared absorption and reflection, tunneling, inelastic neutron scattering, and determination of the conductivities within and perpendicular to the CuO_2 plane.

In response to this need, techniques for growing large single crystals of the cuprate oxide superconductors have been steadily improving, and a variety of significant and, equally important, reproducible experimental results on these samples are now being reported. Nonetheless, there is still considerable room for improvement both in growing single crystals and crystalline films and in quick reliable methods for examining them for such defects as inhomogeneities, multiple phases, weak links associated with phase boundaries, etc. Ideally such methods must be capable of probing the entire sample, a difficult requirement given that the optical opacity of these materials rules out most spectroscopic approaches. Some of the methods that do satisfy this requirement have various drawbacks, as, for example, x-ray and neutron diffraction methods are tedious and lack the sensitivity required to detect small regions of inhomogeneity, while specific heat and other thermodynamic measurements are hard to interpret because of limited theoretical understanding of the cuprate oxide superconductors. The complexities of diffraction methods have been well demonstrated by Cox *et al.*, who used them to detect compositional inhomogeneities in $La_{2-x}M_xCuO_4$ ceramic samples.[2]

Given the foregoing difficulties, the magnetically modulated resistance (MMR) techniques, which have been very useful for characterizing polycrystalline and thin film superconducting samples,[3–6] can play an important role in assessing the quality of crystalline superconductors. This is demonstrated in this paper in which examination of a $(La_{0.94}Sr_{0.06})_2CuO_4$ single crystal sample by two variants of the MMR technique, namely, magnetically modulated microwave absorption (MAMMA),[3,4] and magnetically modulated electrical resistance (MAMER),[5,6] reveals the presence of multiple phases with correspondingly different T_c's, and weak link behavior that probably is due to Josephson tunneling junctions at the interfaces between the different superconducting regions. Although this single crystal is identical in composition and method of growth[7] to a number of crystals used in various experiments,[8–10] it should be clearly noted that this paper deals primarily with the utility of the MMR techniques for detecting such defects and the importance of such examinations of crystals used in critical experiments. Whether these defects are peculiar to this particular crystal or are intrinsic to all crystals of similar composition and method of growth remains to be established.

Finally, it should be noted that, given this quick convenient method for determining the presence of defects in single crystals, it may be possible to obtain useful information by deliberately introducing defects into initially perfect single crystals and correlating the resulting changes in superconducting and other properties with the defects indicated by the MMR measurements.

II. EXPERIMENTAL

The magnetically modulated resistance methods have been extensively discussed in a number of previous publications,[3-5,11] so only a cursory summary of the methods, together with some important considerations when applying them to crystalline samples, is required here. Briefly, these techniques can both unequivocally detect the occurrence of a superconducting transition (or transitions in multiphasic samples) and observe effects due to weak links between phase and/or grain boundaries. This is possible because both the superconducting transition, and the ability of superconducting currents to pass through the weak links are magnetic field dependent. Consequently, application of an oscillating magnetic field produces a corresponding oscillating component in the measured resistance or electromagnetic loss in the sample, which component is readily observed with high sensitivity by conventional narrow band amplification and phase sensitive detection (lockin) techniques. Customarily this magnetically modulated resistance is observed simultaneously with the corresponding unmodulated resistance as a function of temperature.

There is an important difference between the microwave and dc resistance variants of the MMR method. MAMMA is global in that it examines all regions of the sample, at least insofar as the microwaves can penetrate the sample, whereas MAMER yields local information about the best superconducting path or paths through the sample. The resulting ability to obtain complementary information about the sample has proved very useful in a number of instances, as will be illustrated here.

In thin films the MAMMA method is truly global, at least for some orientations, as the film thickness is less than the microwave skin depth. Experimental experience suggests that the MAMMA method also examines a substantial part of most bulk granular samples, most likely because a majority of the individual grains are smaller than the microwave skin depth with enough low conductance regions between the grains to allow penetration of the microwaves in the bulk of the sample.[12,13] The situation will be different, however, for single crystals whose dimensions are larger than the microwave skin depth. Typical skin depths (calculated from the formula $\delta=\sqrt{1/\pi\nu\mu\sigma}$, where ν is the frequency, σ is the conductivity, and μ is the permeability of the sample) are roughly 0.0007 and 0.02 cm at 9.1 GHz for the *ab*-plane and *c*-axis directions, respectively, which values correspond to the conductivities of 8000 and 11 $\text{ohm}^{-1}\,\text{cm}^{-1}$ observed in these respective directions for a ($La_{0.94}Sr_{0.06}CuO_4$) crystal at a temperature just above T_c.[9] Thus, for single crystals the MAMMA response will provide information about the surface region, whereas the dc-resistance-based MAMER response will provide information about the best superconducting path through the sample, which path is likely to be through interior regions of the crystal.

In single crystal studies, where observation of orientation dependent effects can provide significant information, it is important to consider the geometry of the MAMMA experiment, as illustrated in Fig. 1. The sample is located in the center of a rectangular *X*-band microwave cavity operating in the TE_{102} mode, which is the same configuration used in electron spin resonance (ESR) experiments, and the cavity is, in fact, an ESR cavity with built-in field modulation coils. The variable sample temperature is controlled by the flow of He gas from a liquid He reservoir though a Dewar (not shown in the figure) which passes through the center of the cavity in the *X* direction. For the TE_{102} cavity mode the microwave magnetic field (H_{mw}) is as shown by the dotted lines in Fig. 1 with a maximum at the sample position, while the microwave electric field (E_{mw}) lies in the *YZ* plane and has a node at the sample position. The modulating magnetic field ($H_m \sin\omega_m t$) and a dc magnetic field (H_{dc}), which can be of varying strength but is always at least as large as H_m so that the net field never changes sign, are applied along the *Z* axis, i.e., perpendicular to H_{mw}. As the microwave electric field vanishes at the sample, the primary source of microwave loss in the sample is the resistive loss experienced by the eddy currents induced by H_{mw}. For the geometry of Fig. 1 these currents circulate in the *YZ* plane, and the resistive losses are due to the resistances along the two crystal axes which are aligned with the *Y* and *Z* axes for a given sample orientation. Similarly the effects of the dc and modulating fields reflect the changes in the superconductive properties of the sample due to a field applied along that crystal axis which is aligned with the *Z* axis. For the superconducting transition itself this effect is the decrease in T_c with increasing field, which decrease is equivalent to an increase in the external temperature and a corresponding resistance change, as given by the equation[4]

$$\left[\frac{dR}{dH}\right]=\left[\frac{dR}{dT}\right]\left[\frac{dT_c}{dH}\right]. \tag{1}$$

Thus, the MMR response in the vicinity of a superconducting transition will be proportional to dR/dT, which

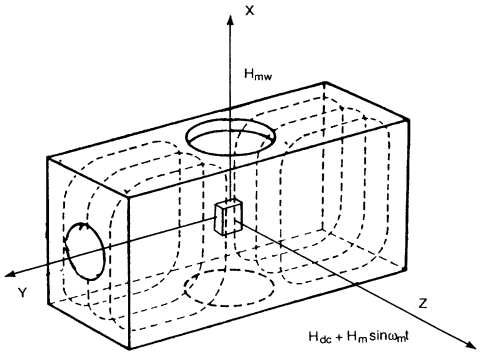

FIG. 1. Illustration of the microwave cavity used in the MAMMA (and MAMER) experiments, including location of the sample, the orientation of the microwave magnetic field (H_{mw}) (dashed lines — — —), and the dc and modulating magnetic fields.

relation should also hold if there are several transitions with slightly different T_c's in a multiphasic sample because dT_c/dH will not differ significantly among these transitions. As will be discussed later, dR/dT is readily calculated from the experimental R versus T data and comparison of this quantity with the observed MMR response can distinguish between the intrinsic response(s) due to the superconducting transition(s) and the weak link responses because the latter are not proportional to dR/dT. Furthermore, the weak link responses usually have stronger magnetic field dependences than do the intrinsic responses, which is another basis for distinguishing between them.

It is important to note that the predominant microwave absorption mechanism, which is dissipation of the microwave-induced eddy currents by sample resistances in the directions of eddy current flow, makes these microwave methods different from low frequency ac susceptibility, even though the results of both can be expressed in terms of a complex magnetic susceptibility. The eddy current losses, being proportional to frequency, are quite small in the low frequency technique, which therefore observes the conventional response of the sample to an applied magnetic field, i.e., effects due to induced magnetic moments and reorientation of existing moments in the sample.

The MAMER experiments are carried out with the sample configured for a four-point probe resistance measurement, and located in the Dewar-cavity apparatus of Fig. 1 for convenience in applying the magnetic field modulation.[5,6] Another advantage of this set-up is that MAMMA and MAMER experiments can be performed consecutively on the same sample. The field modulation frequency in both experiments is 10 kHz (this is not critical and a range of frequencies from 1 to 100 kHz could be used) and the amplitude of the modulating field ranges up to 5 G. In the MAMER experiment the resistance-dependent voltage generated across the sample by the applied current is amplified, phase detected at the modulation frequency, and recorded as a function of temperature. Another parameter in the MAMER experiment is the sample current, as the MAMER response can vary considerably with current, especially if the sample contains current-limiting weak links.[6]

The $(La_{0.94}Sr_{0.06})_2CuO_4$ crystal had dimensions of 1.5, 0.5, and 1.0 mm along the a, b, and c axes, respectively, where a and b denote crystal axes in the CuO_2 plane while c is the crystal axis perpendicular to this plane. It should be noted, however, that a is not necessarily the true a crystallographic axis of the rhombic crystal, but could be either the a or b crystallographic axis and similarly for b.

III. RESULTS AND DISCUSSION

We present first the dc resistance and MAMER results on the $(La_{0.94}Sr_{0.06})_2CuO_4$ crystal, and then compare these results with corresponding microwave and MAMMA experiments. In all MAMER experiments the dc current was directed along the a crystallographic axis as the dimensions of the crystal made it much more difficult to attach leads for currents along the b or c axes. Figure 2 gives the dc resistance and corresponding MAMER response versus temperature for a 1-mA current and dc fields of 30 and 3000 G oriented along both the b and c crystal axes. (For the convenience of the reader, this and all subsequent figures contain an inset showing the orientations of the dc sample current, or H_{mw}, and $\mathbf{H}_{dc}\|\mathbf{H}_m$ with respect to the crystal axes.) These responses are independent of sample current except that the curves are shifted to lower temperature (about 3 K lower at 10 mA current), which effect is probably due to heating of the sample in the normal state so that its actual temperature is somewhat higher than the temperature indicated by the thermocouple.

The dc resistance, shown in Fig. 2(a), indicates a moderately sharp superconducting transition, about 4 K in width, with $T_{c,\mathrm{mid}}=29.4$ K in a small 30 G external field, where $T_{c,\mathrm{mid}}$ is the point where the resistance is half the value just prior to the start of the superconducting transition. Application of a 3-kG field has no observable effect on the width of the transition but lowers $T_{c,\mathrm{mid}}$ to

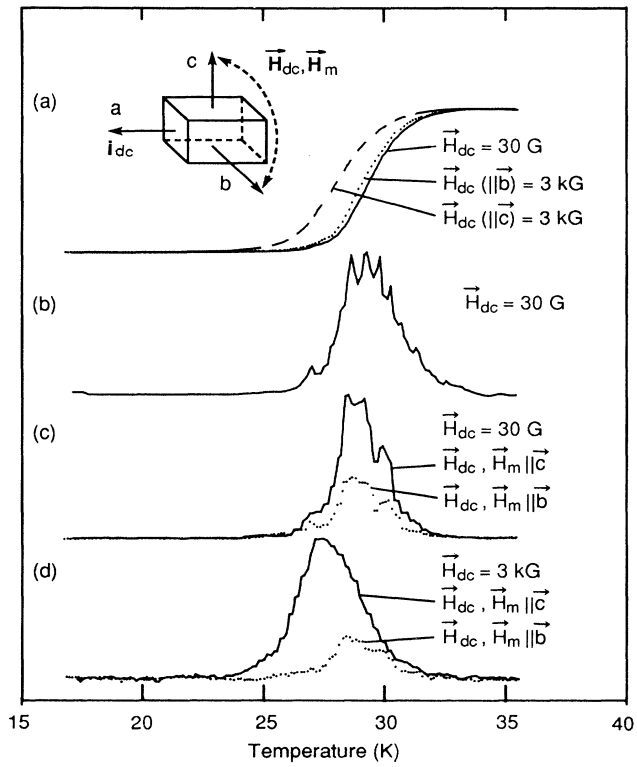

FIG. 2. dc resistance and MAMER vs temperature in the $(La_{0.94}Sr_{0.06})_2CuO_4$ crystal for various strengths and orientations of the external magnetic field, and a 1-mA current along the a axis. (a) dc resistance. (b) dR_{dc}/dT, calculated from the observed R_{dc} vs T for $H_{dc}=30$ G. (c) MAMER response for $H_{dc}=30$ G. (d) MAMER response for $H_{dc}=3$ kG. The inset shows the orientations of the currents and fields with respect to the crystal axes.

29.1 and 28.1 K for H_{dc} parallel to the b and c axes, respectively. This gives $(dT_c/dH)_{\parallel}=-0.10$ K/kG and $(dT_c/dH)_{\perp}=-0.43$ K/kG for fields parallel and perpendicular to the bc conduction plane. These results agree well with the values of $(dT_c/dH)_{\parallel}=-0.08$ K/kG and $(dT_c/dH)_{\perp}=-0.38$ K/kG obtained from the resistance data of Kambe *et al.*[9] for $H_{dc}=5$ kG. It should be noted that the magnitudes of the dT_c/dH decrease rapidly with increasing field; the data of Kambe *et al.*[9] give an average $(dT_c/dH)_{\parallel}=-0.04$ K/kG and $(dT_c/dH)_{\perp}=-0.16$ K/kG over a 50-kG field interval. These strong dependences on field orientation and magnitude may account for the fact that results for dT_c/dH in polycrystalline samples of the $(La_{1-x}Sr_x)_2CuO_4$ superconductors vary considerably and generally are smaller (some typical values are -0.08 K/kG,[14] and -0.2 K/kG,[15]) than the values found here.

Although the dc resistance data showed a moderately sharp, structureless superconducting transition, the MAMER response, shown in Fig. 2(c) for $H_{dc}=30$ G, contains at least four peaks, which we interpret as indicative of a multiphasic crystal with regions of somewhat different T_c. The shape of the MAMER response is independent of the orientation of H_{dc}, and H_m which is parallel to H_{dc}, but the response is considerably stronger for $H_m \| c$ than for $H_m \| b$, as expected from Eq. (1) because $|dT_c/dH|_{\perp} > |dT_c/dH|_{\parallel}$. Although weak links in the superconducting current path also can yield MMR responses like those in Fig. 2(c), in which the peak(s) below the intrinsic peak at T_c are due to the weak links,[6] the multiphasic interpretation is favored here for several reasons. One reason, as discussed following Eq. (1), is that dR_{dc}/dT calculated from the experimental R_{dc} versus T data, and shown in Fig. 2(b), generally matches the shape of the MAMER response around T_c, although the comparison is only qualitative because small uncertainties in the temperature measurement lead to larger "noiselike" uncertainties in the calculated dR_{dc}/dT. As noted previously, this relationship will not hold if weak links contribute significantly to the MMR response because the weak link responses are not proportional to dR_{dc}/dT, and, furthermore, they usually have stronger magnetic field dependences than do the intrinsic responses.[6] Another reason is the aforementioned observation that increasing the sample current shifts the MAMER response to lower temperature but does not change its overall shape, whereas large shape changes were observed in a sample known to contain weak links.[6] A second reason is that, as shown in Fig. 2(d), the overall shape of the MAMER responses in the higher field of 3 kG are little changed from those observed at 30 G, even though the response for $\mathbf{H}_{dc} \| \mathbf{c}$ is noticeably shifted to lower temperature and the number of distinct peaks in it are reduced, probably because of slight field broadening of the individual MAMER peaks. Again, this is the expected result for a multiphasic sample whose slightly different superconducting regions should have the same magnetic field dependence, whereas, the magnetic field dependences of the weak link peaks usually differ significantly from that of the intrinsic peak. Finally, it may be noted that the MAMER responses at 3 kG are about fives times weaker than their 30-G counterparts, which reflects the marked decrease in $|dT_c/dH|$ with increasing field, and, as observed previously, the response for $\mathbf{H}_m \| \mathbf{c}$ is considerably stronger than that for $\mathbf{H}_m \| b$.

The microwave results shown in Fig. 3 for $\mathbf{H}_{mw} \| \mathbf{a}$ and $H_{dc}=30$ G are interestingly different from the dc resistance and MAMER results. The microwave absorption, expressed in terms of a microwave resistance (R_{mw}) is shown in Fig. 3(a). It gives $T_{c,mid}=26.5$ K, versus 29.4 K from the dc measurement, and the transition is considerably broader than its dc counterpart. The corresponding MAMMA response, shown in Fig. 3(c), contains two broad peaks centered around 27.2 and 24.6 K with some indications of distinct subpeaks within the broad peaks. Again, this structure is interpreted as due to different phases with different T_c's, which is supported by the good agreement between the MAMMA response and the calculated dR_{mw}/dT shown in Fig. 3(b). Just as was found in the MAMER experiment and attributed to the field-orientation dependence of dT_c/dH, the MAMMA

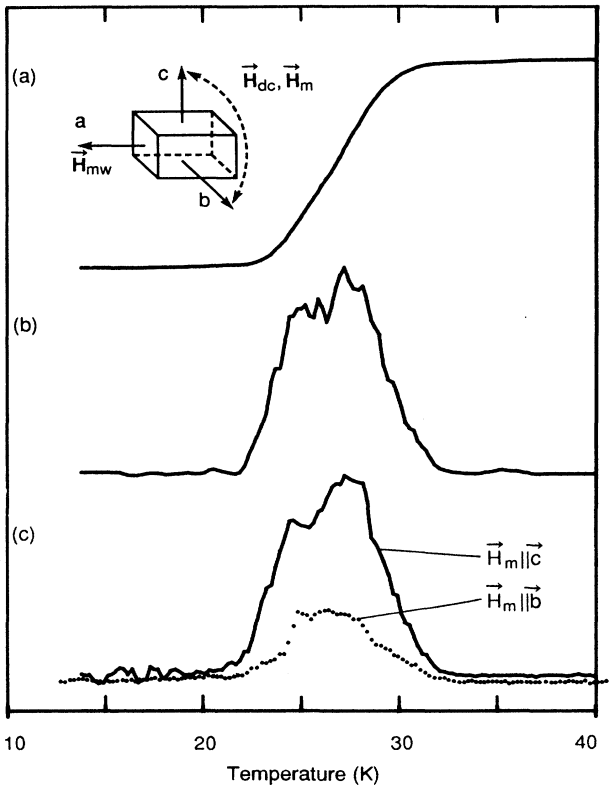

FIG. 3. Microwave resistance and MAMMA vs temperature for the $(La_{0.94}Sr_{0.06})_2CuO_4$ crystal for $H_{dc}=30$ G and two orientations of the modulation field, with the microwave magnetic field along the a axis. (a) Microwave resistance. (b) dR_{mw}/dT, calculated from the observed R_{mw} vs T. (c) MAMMA response. The inset shows the orientations of the microwave, dc, and modulating magnetic fields with respect to the crystal axes.

response is considerably stronger for $\mathbf{H}_m \| \mathbf{c}$ than for $\mathbf{H}_m \| \mathbf{b}$, as shown in Fig. 3(c). The effect of a 3-kG field on R_{mw} and the MAMMA response is similar to that found for R_{dc} and the MAMER response.

That the dc resistance and MAMER response should indicate a higher quality superconductor than does the microwave loss and MAMMA is not surprising because, as noted previously, the former samples the best superconducting path through the sample whereas the latter samples predominantly the surface regions of the single crystal. Many of the factors which decrease the quality of a superconductor such as inhomogeneous doping, oxygen loss, etc., are likely to affect surface regions more than the bulk of the material. Unfortunately, the surface regions are critical for many experiments, and this result indicates the importance and utility of the MAMMA method for investigating surface quality.

The microwave power dependence of both direct microwave absorption and the MAMMA response is another useful aspect of this microwave technique. As applied to the $(La_{0.94}Sr_{0.06})_2CuO_4$ crystal in the geometry of Fig. 4 with $H_{dc}=30$ G, the results, shown in Fig. 4, add to the evidence that this is a multiphasic crystal with regions of different T_c. As the microwave power is increased, both the drop in the direct microwave absorption and the MAMMA response sharpen and shift downward to the lowest T_c, that is the low-temperature edge of the low-microwave-power MAMMA response shown in Fig. 4(a). The interpretation of this observation is that at higher microwave power the surface regions of the crystal are heated sufficiently to keep the actual temperature of the crystal above the external temperature recorded by the thermocouple. Consequently, the superconducting transition temperature appear to decrease. Furthermore, at the highest microwave powers the heating due to microwave absorption in the lowest T_c regions is sufficient to keep the overall crystal temperature above even the highest T_c, with the result that there are no indications of a superconducting transition until the external temperature equals the lowest T_c. At this point microwave heating ceases as this lowest T_c region goes superconducting together with the higher T_c regions. As microwave heating of the different superconducting regions is likely to be significantly different from heating of weak link regions, this microwave power dependence should be useful for distinguishing between complex MAMMA responses due to multiphasic samples with different T_c's, as is the case here, and those due to the presence of weak links.

The foregoing results show little or no indication of weak links effects either for $\mathbf{i}_{dc} \| \mathbf{a}$, or $\mathbf{H}_{mw} \| \mathbf{a}$, in which latter case the microwave eddy currents circulate along the b and c axes, partly in and partly out of the conduction plane. However, MAMMA data indicates a strikingly different situation when $H_{mw} \| \mathbf{c}$ so that the microwave eddy currents circulate along the a and b axes, entirely in the conduction plane. Although the microwave resistance, shown for this geometry with $H_{dc}=30$ G in Fig. 5(a), is unremarkable, being only somewhat broader than found for $H_{mw} \| \mathbf{a}$ [cf. Fig. 3(a)] and independent of the orientation of H_{dc} in the ab conduction plane, the MAMMA response, shown in Fig. 5(c), has several novel features, the most obvious of which is the strong dependence on the orientation of H_{dc}, and/or H_m, which is parallel to it. For $\mathbf{H}_{dc}, \mathbf{H}_m \| \mathbf{b}$ the MAMMA response generally resembles the calculated dR_{mw}/dT, shown in Fig. 5(b), however, the lower temperature peak at 22.2 K in the MAMMA response is significantly below the corresponding lower temperature peak at 23.5 K in dR_{mw}/dT. Also, below about 18 K there is a slowly increasing tail in the MAMMA response which has no counterpart in dR_{mw}/dT. As H_{dc} and H_m are rotated in the ab plane, the intensity of this 22.2-K peak increases markedly and shifts to slightly lower temperatures, while the higher temperature portions of the MAMMA response are relatively unaffected. Increasing H_{dc} to 1 kG decreases the intensity of the lower temperature MAMMA peak somewhat relative to the intensity of the higher temperature peak, and markedly decreases the nonzero tail in the MAMMA response. These observations are strong evidence that the peak between 21 and 22 K and the tail below 18 K are due to some type of weak link encountered by superconducting currents flowing in the conduction plane. Furthermore, the fact that the

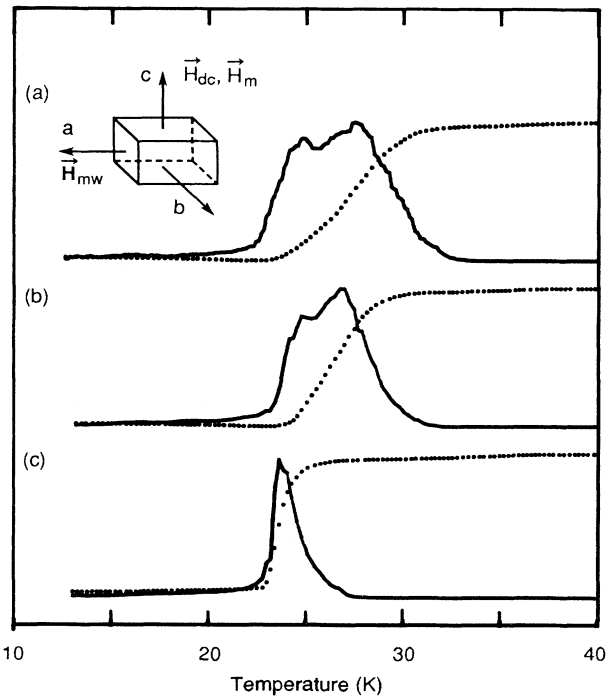

FIG. 4. Microwave power dependence of the microwave resistance (dotted curves) and MAMMA response (solid curves) for the $(La_{0.94}Sr_{0.06})_2CuO_4$ crystal with H_{mw} parallel to the a axis, and $H_{dc}=30$ G parallel to the c axis. (a) Low microwave power. (b) Microwave power six times greater than in (a). (c) Microwave power 16 times greater than in (a). The inset shows the orientations of the microwave, dc, and modulating magnetic fields with respect to the crystal axes.

21–22-K peak is most intense for $\mathbf{H}_{dc},\mathbf{H}_m\|\mathbf{a}$ indicates that the associated weak link is oriented so as to be encountered by currents flowing along the b axis, because it is difficult to envision a supercurrent flowing through a weak link being affected by a magnetic field parallel to this current.

This result is not surprising given the multiphasic character of the sample with the attendant likelihood of weak links associated with boundaries between phases. Although the present data are insufficient to fully identify the nature of these weak links, the observed changes with only a moderate increase in magnetic field are a strong indication that Josephson junctions between different superconducting regions contribute to some extent.[6,13] Furthermore, the strong dependence of the weak link responses on magnetic field orientation requires that the postulated Josephson junctions be preferentially oriented, as recently observed for Josephson junctions in the organic superconductor κ-$(BEDT\text{-}TTF)_2Cu(NCS)_2$.[16] Specifically, the prominence of the weak link effects for $\mathbf{H}_{mw}\|\mathbf{c}$ and $H_{dc},\mathbf{H}_m\|\mathbf{a}$ requires that the Josephson junctions lie predominantly along the b axis, as this maximizes the flux through the junction when $\mathbf{H}_{dc}$ and $\mathbf{H}_m$ are along **a**. This orientation readily accounts for the absence of weak link effects in the dc resistance and MAMER results for $\mathbf{i}_{dc}\|\mathbf{a}$ (Fig. 2), and the microwave and MAMMA results for $\mathbf{H}_{mw}\|\mathbf{a}$ with $\mathbf{H}_{dc},\mathbf{H}_m\|b$ (Fig. 3). The apparent absence of weak link effects from the MAMMA response for $\mathbf{H}_{mw}\|\mathbf{a}$ and $\mathbf{H}_{dc},\mathbf{H}_m\|\mathbf{c}$ (Fig. 3), which geometry also maximizes the magnetic flux through b-axis oriented Josephson junctions, is likely due to the decreased prominence of the weak link response relative to the intrinsic MAMMA response for this geometry. The reasons for this are twofold. One is that the intrinsic MAMMA response is largest, and thus tends to obscure the weak link response, for H_m in the conduction plane where $|dT_c/dH|$ is largest [cf. Eq. (1)]. The second is that the postulated Josephson junctions will have a greater effect on current flow that is entirely along the ab conduction axes than for a current flow that is partly along the c axis where the weak coupling between the ab planes is a competing impediment to current flow.

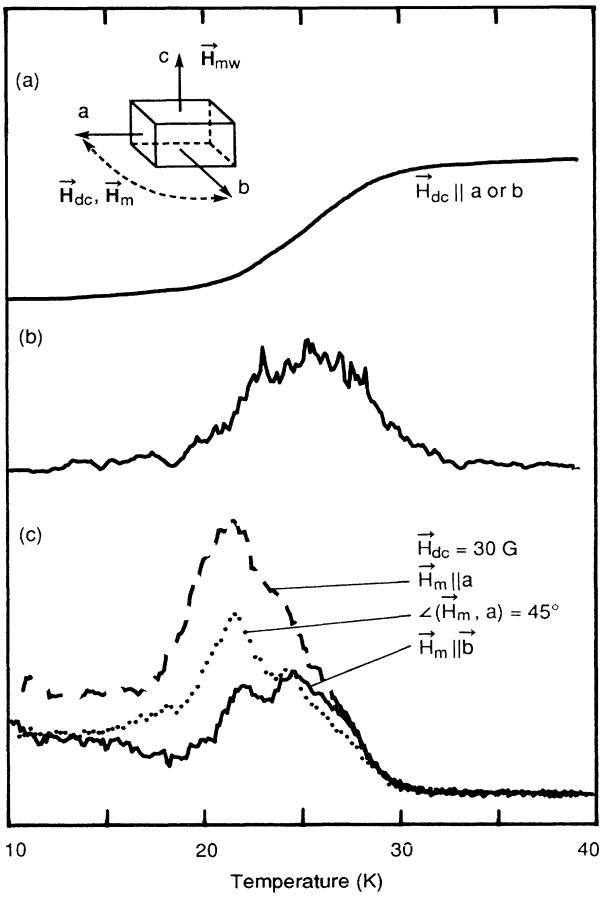

FIG. 5. Microwave resistance and MAMMA vs temperature for the $(La_{0.94}Sr_{0.06})_2CuO_4$ crystal for $H_{dc}=30$ G and several orientations of the modulation field, with the microwave magnetic field along the c axis. (a) Microwave resistance for $H_{dc}\|a$ or b. (b) dR_{mw}/dT, calculated from the observed R_{mw} vs T. (c) MAMMA response. The inset shows the orientations of the microwave, dc, and modulating magnetic fields with respect to the crystal axes.

In summary, the present results indicate that magnetically modulated microwave and dc resistance measurements, particularly when made in conjunction with measurement of the corresponding direct resistances, constitute a simple and versatile method of examining single crystals of superconductors for a variety of defects. As noted in the Introduction, it remains to be determined whether or not the defects found in this particular $(La_{0.94}Sr_{0.06})_2CuO_4$ crystal are inherent in the processes of doping and/or growing crystals of this composition. An important related question is whether near-atomic-scale variations in the dopant or oxygen concentrations play a role in the multiphasic superconductive behavior observed here because such inhomogeneities are unavoidable in the case of dopants and are quite likely in the case of the labile oxygen component. Screening of superconductor crystals for the types of defects found here may help answer the foregoing very important questions, in addition to assuring that the best possible crystals are used in critical experiments.

ACKNOWLEDGMENTS

The authors are pleased to acknowledge the receipt of the single crystal of $(La_{0.94}Sr_{0.06})_2CuO_4$, which was grown at the Institute of Organic Synthesis, Yamanashi University, Kofu, by Professor I. Tanaka and H. Kojima, and which was kindly sent to us by Professor K. Kitazawa of the University of Tokyo. This work was supported by the Department of the Navy, Space, and Naval Warfare Command, under Contract No. NO0039-89-C-0001.

[1]Proceedings of the International Conference on High-Temperature Superconductors [Physica C **151-153** (1988)] is a good summary of the present situation.
[2]D. E. Cox, S. C. Moss, R. L. Meng, P. H. Hor, and C. W. Chu, J. Mater. Res. **3**, 1327 (1988).
[3]K. Moorjani *et al.*, Phys. Rev. B **36**, 4036 (1987).
[4]B. F. Kim, J. Bohandy, K. Moorjani, and F. J. Adrian, J. Appl. Phys. **63**, 2029 (1988).
[5]J. Bohandy, T. E. Phillips, F. J. Adrian, K. Moorjani, and B. F. Kim, Mod. Phys. Lett. B **3**, 933 (1989).
[6]B. F. Kim, J. Bohandy, T. E. Phillips, F. J. Adrian, and K. Moorjani, Physica C **161**, 76 (1989).
[7]I. Tanaka and J. Kojima, Nature (London) **337**, 21 (1989).
[8]K. Kitazawa, S. Kambe, M. Naito, I. Tanaka, and H. Kojima, Jpn. J. Appl. Phys. **28**, 55 (1989).
[9]S. Kambe, M. Naito, K. Kitazawa, I. Tanaka, and H. Kojima, Physica C **160**, 243 (1989).
[10]G. Shirane *et al.*, Phys. Rev. Lett. **63**, 330 (1989).
[11]K. Moorjani, B. F. Kim, J. Bohandy, and F. J. Adrian, Rev. Sol. State Sci. **2**, 263 (1988).
[12]J. Bohandy, J. Suter, B. F. Kim, K. Moorjani, and F. J. Adrian, Appl. Phys. Lett. **51**, 2161 (1987).
[13]J. Bohandy, B. F. Kim, F. J. Adrian, and K. Moorjani, Phys. Rev. B **39**, 2733 (1989).
[14]J. M. Tarascon, L. H. Greene, W. R. McKinnon, G. W. Hull, and T. H. Geballe, Science **235**, 1373 (1987).
[15]R. J. Cava, R. B. van Dover, B. Batlogg, and E. A. Reitman, Phys. Rev. Lett. **58**, 408 (1987).
[16]J. Bohandy, B. F. Kim, F. J. Adrian, K. Moorjani, S. D'Arcangelis, and D. O. Cowan, Phys. Rev. B **43**, 3724 (1991).